A Multi-Mode Pattern Diverse Microstrip Patch Antenna Having a Constant Gain in the Elevation Plane

Kamil Karaçuha[1], Feza Turgay Çelik[2], and Halil Ismail Helvaci[3,4]
[1]Electrical Engineering Department, Istanbul Technical University, Istanbul, Turkey
[2]Department of Electrical and Electronics Engineering, Faculty of Engineering, Middle East University, Ankara, Turkey
[3]Satellite Communication and Remote Sensing, Informatics Institute, Istanbul Technical University, Istanbul, Turkey
[4]Department of Electrical and Computer Engineering, University of Kentucky, Lexington, Kentucky, USA

Corresponding author: K. Karaçuha (e-mail: karacuha17@itu.edu.tr)

ABSTRACT This study investigates a multi-mode pattern diverse microstrip patch antenna operating at 2.45 GHz. The study aims to have a flat top gain covering more than 90^0 in the elevation plane to provide equal service quality to everyone in the region of interest. In order to achieve such a crucial goal, the cavity model approach for the rectangular patches is employed. TM_{01} and TM_{02} modes are selected for the design since their corresponding radiation patterns are suitable for scanning a wide range. The superposition of boreside and conical (monopole-like) beams form a wide beam radiation pattern in elevation. Coupling between different modes is reduced by placing two radiators perpendicular to each other. In addition, the design aims to reduce both initial dimensions of the antenna by using fractalization, slotting, and perpendicular positioning techniques. These techniques reduce the original dimension of the design to less than its 60%. The simulation and experimental results reveal many similarities regarding the scattering parameters, radiation patterns, and gain. The scattering parameters, $|S_{11}|$ and $|S_{22}|$ at the operating frequency, are less than -10 dB, and the wide beam radiation pattern (more than 90^0) is obtained in the elevation plane.

INDEX TERMS Antenna Design, Miniaturization, Mode analysis, Wide Beam Radiation, Flat-top Beam

I. INTRODUCTION

INCREASING demand on connectivity, entertainment, and leisure time requires handling many tasks, prioritizing the investigation of antenna design and manufacturing. The researchers' key points are the radiation pattern reconfigurability, compactness, energy efficiency, eco-friendly production, and equal distribution to end-users. From the technical point of view, beyond such criteria, different parameters should also be taken into account, such as theoretical limits, manufacturability, insensitivity to manufacturing errors, and arraying of unit cells [1], [2]. Due to many factors related to the change in preferences and choices of personal lifestyle, people spend more time indoors compared to the previous decades. Therefore, usage of indoor applications, the internet of things (IoT), and 5G would be more progressive and fast compared to its previous technological revolutions [1]–[4].

For achieving the aforementioned technological steps, the antenna plays a critical and crucial role on the stage. The antenna design for a new generation of technology is a vital topic for both academic and commercial interests. Therefore, the present study aims to design an antenna that can be employed in indoor applications. Remarkably, a new miniaturized microstrip patch antenna with wide beam radiation characteristics at 2.45 GHz is proposed. The motivation behind such radiation characteristics is to provide each end user equal service quality by flattening radiation characteristics in the region of interest. In other words, the radiated power in an elevation ($\pm 45^0$) angle interval should be constant.

In recent work, one of the deeply studied antenna structures is the microstrip patch antenna due to its simplicity of design, ease of integration with other circuits, minimum weight, and low cost. Authors in [5] designed a wideband microstrip patch antenna for 5G wireless applications, with an antenna gain of 5.22 dB etched on Rogers RT5880 substrate with a compact size of 20 x 20 mm^2 with a thickness of 0.79 mm. Design in [6] has a similar patch antenna etched on Rogers RT5880 substrate that can cover the WiMAX, WLAN, and S-band range using an antenna with dimensions 60mm x 55mm x 1.59 mm^2. Research in [7] demonstrates a microstrip patch antenna design with dimensions of 38mm x 29mm x 0.13 mm, successfully integrated into 2.4 GHz Wireless Communication Applications.

In the literature, a vast number of studies related to pattern reconfigurability and radiation diversity exist [8]–[16]. Mainly, there are three approaches [3]. The first approach is to employ parasitic elements in the design. The second

approach is to operate simultaneously or consecutively different cavity or characteristics modes, and the last method is inserting multiple radiating elements [8], [12], [17]. Respectively, in the first approach, the primary purpose of including a parasitic element in the design leads to having the ability to control the beam where the direction of the steering is determined by the relative dimension and orientation of the parasitic elements [8]–[11]. Apart from the first approach, cavity modeling of the patch antenna types reveals the radiation mechanism of the antenna structure from a different perspective [12]–[15]. Each mode has its characteristic radiation pattern, and combining these different modes can allow having reconfigurable or diverse radiation characteristics. Lastly, by including more than one radiation unit, called subelements of the antenna unit cell, the steerable and diverse radiation pattern can be obtained [17]–[21]. In [22], [23], again, the multimode excitation is employed. With multiple excitations to co-centric circular and ring patches. Several radiation characteristics are obtained. By changing the phase of the excitations, the different modes are stimulated.

In the present study, the cavity model approach is preferred since the two modes of the patch antenna are excited to achieve the required radiation pattern. Then, the antenna is miniaturized to have a suitable unit cell for arraying, including slots and fractals. This study aims to design a linearly-polarized microstrip patch antenna operating at 2.45 GHz (for Wi-Fi), satisfying pattern diversity property. Besides, it needs to be suitable as a unit cell in an array structure (the largest dimension of the design should not exceed λ_0 (λ_0 is the free-space wavelength)). An unequal power divider feeds the two antennas. This leads to pattern diversity since the proposed structure has three different radiation pattern characteristics due to having two feedings. One of the main objectives of the antenna is to obtain a wide beam radiation pattern with a planar antenna structure. Two specifically chosen modes are employed in the structure simultaneously to achieve such an objective. The total radiation pattern becomes flattened in a specific elevation angle interval by combining the modes having broadside and conical radiation beam characteristics. Due to constrain on arraying, the structure is miniaturized by utilizing the concept of fractals and slotting [3]. This miniaturization is done by considering the current density flow on the patches. Here, the goal is to increase the surface current flow path in a smaller region without distorting the present modes. However, miniaturization reduces the antenna dimension, so the coupling, interference, and distortion in mode characteristics become dominant. The patches are located orthogonally in space to eliminate interference (to isolate). Parametric analysis for each step (cavity modes, miniaturization, isolation) is performed to understand the effect of antenna dimensions and structure on its performance. Then, the prototype is produced, and measurements of scattering parameters, radiation patterns, and gain values are done. Experiments validate the simulation.

The structure of the study is as follows. In Section II, the theoretical background of the antenna structure is given. The cavity model, miniaturization, and the approach to increase the isolation are explained in detail in the section. Then, the simulations in Ansys HFSS and their results are given in Section III, where the discussion on the approaches is provided with the parametric investigation. Lastly, the conclusion will be drawn in Section IV.

II. ANTENNA DESIGN

In this section, the design approach and the main theory utilized in the design procedure, the geometry of the antenna, and the miniaturization approaches are provided in detail.

A. THEORY

The purpose of the study is to design an antenna element that results in approximately constant radiated power between $+45^0$ and -45^0 in the elevation. To achieve such a goal, two different radiation patterns are combined. These patterns are named broadside and conical-shaped patterns, respectively. Within these patterns, the broadside radiation focuses its maximum power towards 0^0 in elevation. This radiation pattern has a narrow beam width. On the other hand, the conical beam focuses its radiation towards $\pm 40^0$ in elevation [3], [24]. Therefore, this radiation pattern is also named as monopole-like radiation pattern [13]. In the proposed approach, these radiation patterns are superposed with proper weights to obtain a broadband antenna that has almost constant gain at the entire -45^0 to $+45^0$ range in the elevation.

First, the antenna type is chosen as a microstrip patch antenna. The advantages of the ease of fabrication, low cost, and low profile nature of the patch-type antenna supported this choice, as mentioned previous section. In order to operate with different radiation patterns, different Transverse Magnetic (TM) modes of the rectangular patch antenna are studied. Cavity model solutions of the microstrip antennas reveal different radiation patterns associated with the different TM modes. In the cavity model solution, the upper and lower boundaries of the antenna are assumed as Perfect Electric Conductors (PEC) while the side walls are modeled as Perfect Magnetic Conductors (PMC). This modeling enables the expression of the E-fields inside the rectangular cavity as [3], [24];

$$\begin{aligned} E_z &= E_0 \cos\left(\frac{\pi n x'}{L}\right) \cos\left(\frac{\pi m y'}{W}\right) \\ H_y &= H_0 \sin\left(\frac{\pi n x'}{L}\right) \sin\left(\frac{\pi m y'}{W}\right) \\ E_x &= E_y = H_x = H_z = 0 \end{aligned} \tag{1}$$

where $x' = x + \frac{L}{2}, y' = y + \frac{W}{2}$.

Here, L and W stand for the dimensions of the rectangular patch. In (1), n and m are integers $(0, 1, 2, 3\ldots)$. Note that these numbers cannot be equal to 0 at the same that. Here, (1) has various solutions depending on the integer values of n and m. These different solution sets are denoted as TM modes of the microstrip antenna and depicted as TM_{mn}. The radiation phenomenon can be understood by inspecting

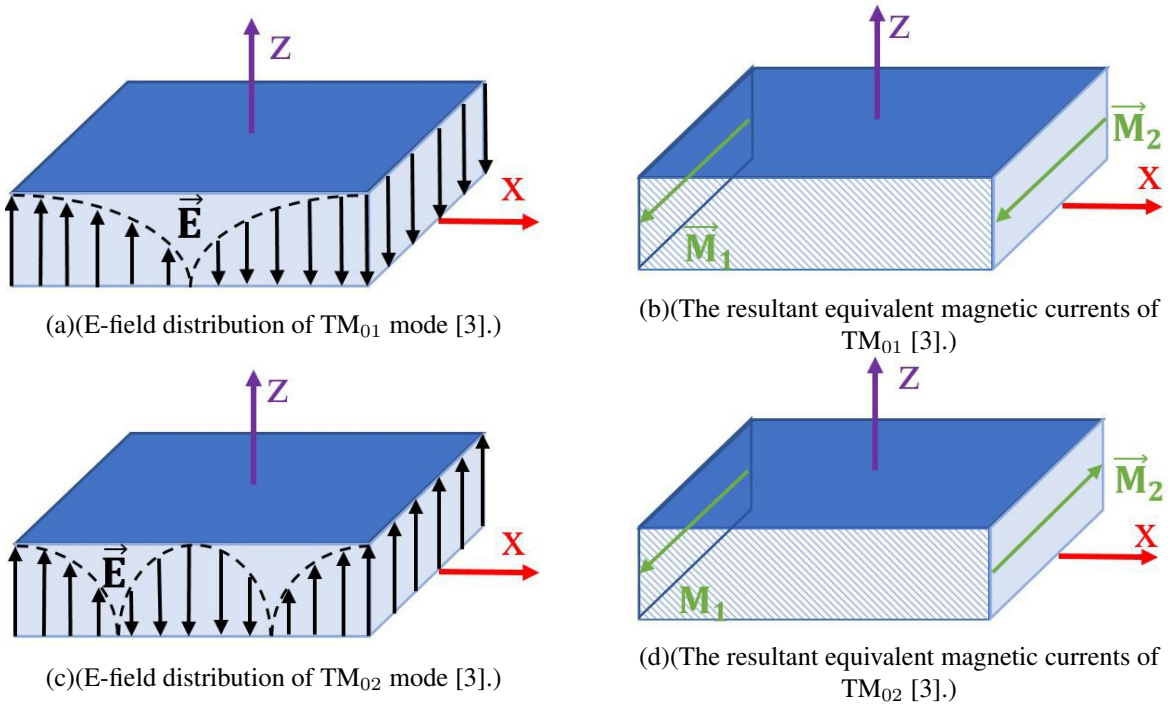

(a)(E-field distribution of TM_{01} mode [3].)

(b)(The resultant equivalent magnetic currents of TM_{01} [3].)

(c)(E-field distribution of TM_{02} mode [3].)

(d)(The resultant equivalent magnetic currents of TM_{02} [3].)

FIGURE 1. Electric field and equivalent radiating current distributions of TM_{01} and TM_{02} modes.

radiating equivalent currents. The E-field distribution and equivalent magnetic currents of the radiating edges of TM_{01} mode can be seen in Figure 1a and 1b [3].

The magnetic current sources at TM_{01} operation constructively interfere at $\theta = 0^0$ direction. Therefore, this mode results in broadside radiation. On the other hand, Magnetic currents of the TM_{02} mode are inversely directed. Therefore, the radiated fields from these sources cancel each other in the broadside direction [3], [24]. Therefore, monopole-like radiation is observed. The E-field distribution of TM_{02} mode and its equivalent magnetic currents can be seen from Figure 1c and 1d [3].

B. ANTENNA GEOMETRY

The antenna geometry consists of two independent microstrip antennas located such that their phase center coincides. The top view of the antenna can be seen in Figure 2. The dimensions in the antenna design are given in Table 1.

As illustrated in Figure 1b and Figure 1d, two edges of the rectangular microstrip antenna are equivalent to the radiating current sources for TM modes. In our geometry, radiating edges are shorter edges of the rectangular patch antenna. The purpose of the design is to obtain an antenna that has broad radiation in the elevation plane; therefore, the phase centers of the two radiations should be coincided. Although creating a co-centric layout yields desired radiation pattern, it introduces excess amount of coupling between radiators. Drastic coupling between elements reduces the radiation efficiency. Radiators are placed orthogonally to increase isolation between them. The top view of the co-centric antenna structure can be seen in Figure 2.

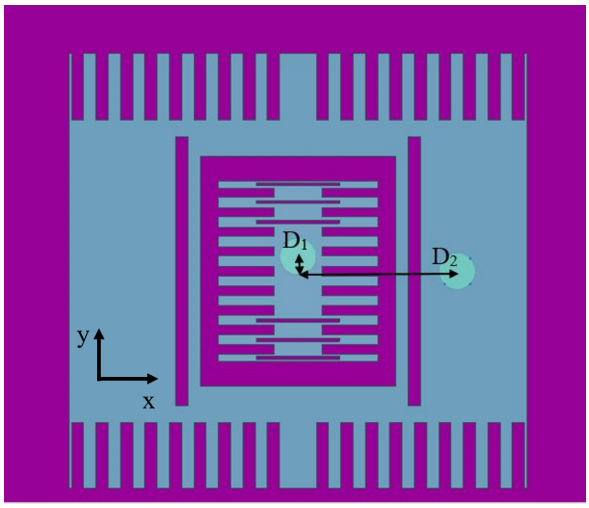

FIGURE 2. Top view of the antenna.

The antenna employs two rectangular-shaped patches as seen in Figure 2. In this design, the inner element is optimized to radiate at TM_{01} mode while the outer patch is arranged so that it radiates in TM_{02} mode. Antenna elements are physically independent of each other. Therefore, they support an independent feed structure. These feed structures are selected as a coaxial probe-type connection (SMA connection) because such a type of excitation is easier to match compared

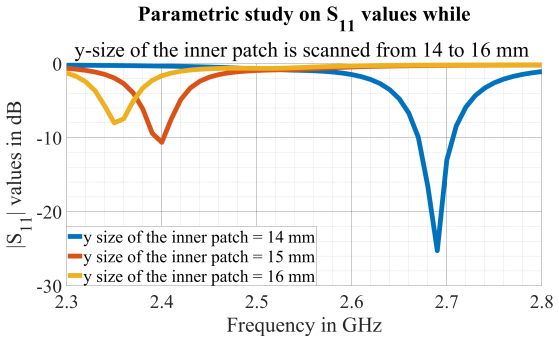

FIGURE 3. Parametric study on $|S_{11}|$ with respect to y size of the inner resonator .

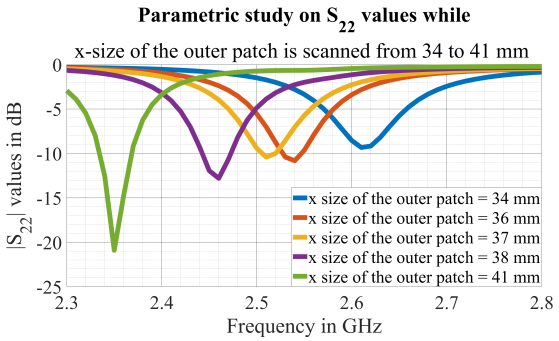

FIGURE 4. Parametric study on $|S_{22}|$ with respect to x size of the outer resonator.

to the other structures. The top view and the feeding points of the antenna can be seen in Figure 2. Throughout the study, the excitation of the inner rectangle is denoted as Port 1, while the excitation of the outer rectangle is denoted as Port 2. Both TM_{01} and TM_{02} modes support dominant currents at their longer edges; therefore, the resonance frequency is mainly determined by the size of the longer edges. The parametric study on the y size of the inner patch and the x size of the outer patch illustrates a relation between resonance frequency and patch edge length as seen in Figure 3 and Figure 4.

The resonance frequency of the inner radiator (operating in TM_{01} mode) increases with a decrease in the y size of the inner patch. The resonance frequency of the TM_{02} mode is also arranged by a similar procedure. The dominant surface currents of the TM_{02} mode are excited in the x direction on the outer radiator. The resonance frequencies of the antenna shift the higher frequencies when the surface currents are limited by reducing the y and x sizes of the radiators, as seen in Figure 3 and 4. This behavior is quite expected and will be benefited the miniaturization process of the antennas. Further geometrical parameters of the antennas will be investigated in the antenna miniaturization part.

Another important measure illustrated in Table 1 is the positions of the feed connection points. The dimension related to feeding structures is determined by considering the impedance matching of the antenna. The antenna edges are

TABLE 1. Parameters and their dimensions

Parameter	Dimension (in mm)
x size of the outer patch	37.4
y size of the outer patch	35.50
x size of the inner patch	13
y size of the inner patch	14.75
x size of the cavity between inner and outer patches	16
y size of the cavity between inner and outer patches	18.75
x size of the slots at the outer patch	1
y size of the slots at outer patch	22
distance between centers of the slots at outer patch	19
x size of slots at the inner patch	6.80
y size of slots at the inner patch	0.25
x size of fractals in the outer patch	1
y size of fractals in the outer patch	5.40
x size of fractals in the inner patch	4.60
y size of fractals in the inner patch	0.75
D_1	1.20
D_2	13
Substrate (& Ground) Size (FR-4 with $\epsilon_r = 4.4$)	140×140

arranged to obtain resonances at 2.45 GHz. Fractal fingers and stubs are tried to be kept as large as possible without the distributing radiation pattern. Therefore, extensive parametric studies are realized to tune the position of the feeding points to match the antennas at the required center frequency.

C. TM MODE GAINS AND WEIGHTING OF THE ANTENNA SUB-ELEMENTS

The main purpose of this design is to obtain an antenna that is capable of producing a radiation pattern that has a very large beam width (90^0) in one principal plane. To achieve this goal, two different radiation patterns are tried to be superposed. This superposition process is carried out so that the phase center of two different TM modes is located at the same point. When the gain values of TM_{01} and TM_{02} modes at the rectangular antenna are investigated, a 3.8 dB gain difference between modes is discovered. This difference between modes is expected. Since the conical beam illuminates $+40^0$ and -40^0 in elevation with two different beams, the gain value of this mode is expected to be smaller than the broadside direction (it only focuses radiation towards one direction). The gain difference between modes is solved by an unequal power divider. In order to superpose two radiation patterns having the same gain, Port 1 (inner patch) is excited with input power less than 3 dB with respect to Port 2 (outer patch). The division between two ports is provided by the unequal power divider.

D. ANTENNA MINIATURIZATION

The IoT and wireless server applications rely on multi-input and multi-output (MIMO) technology. Therefore, the antenna elements of these operations must be compatible with the array structures. In order to fit in the regular array topology, the antenna element must be smaller than $\lambda_0/2$ in the direction of arraying. When none of the miniaturization techniques are applied to the antenna, the size of the outer rectangle along the x-direction becomes 65 mm (0.53λ). The

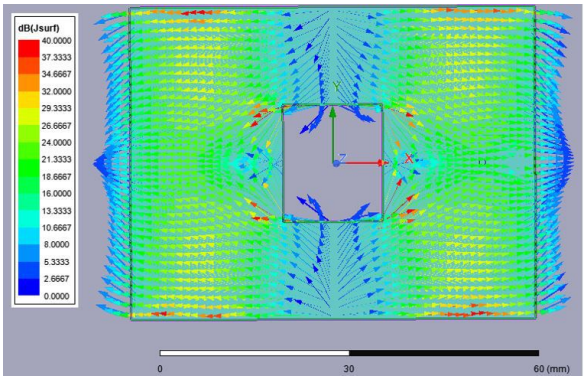

FIGURE 5. Surface currents of the antennas: non-miniaturized case.

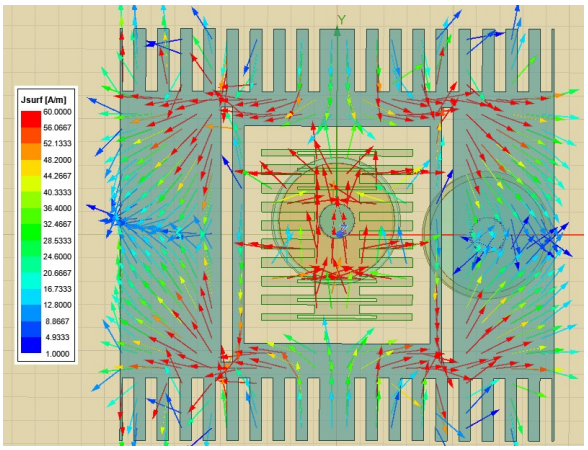

FIGURE 6. Surface currents of the antennas: miniaturized case.

size of the original design is vast for array operations. Thus, two different techniques are employed to reduce the antenna size. One of these methods is the fractionalization of the non-radiating edges of the antenna. The primary purpose of this method is to increase the path on which the surface current travels. The finger-type structure of edges introduces a different surface. Therefore, they increase the edge length of the antenna [24]. The advantage of the fractal structure is more dominant if a significant portion of the surface currents follow the longer path provided by fractals. At this point, the second miniaturization technique is necessary to guide the surface currents. This second miniaturization technique is slot employment. As it can be seen from Figure 2, both inner and outer rectangular antenna has a pair of slots. Besides, there are additional slots at the inner rectangle patch. These slots are employed to force surface currents to use fractal paths [24]. The surface currents with and without using the miniaturization techniques can be seen in Figures 5 and 6.

As seen in Figure 5, currents follow straight edges in TM_{02} mode. This behavior is changed by the fractalization of edges and slot employment. The effect of these methods increases the length of the current and resonates with the antenna at a lower frequency. In this design, by applying miniaturization, the length of the antenna along the x-direction is reduced to 37.4 mm ($0.3\lambda_0$). Thus, the size of the miniaturized antenna is suitable for the regular array topology. A similar miniaturization scheme is also applied to the inner resonator. As it operates in TM_{01} mode the dominant surface currents flows in the y-direction. The fractal fingers and slots are etched to force current to flow in the y-direction by extending its path. The current distribution after miniaturization can be seen in Figure 6.

In Table 2, a comparison with several studies is provided. The proposed antenna is compared to other studies designed with similar approaches. The advantage of this study is to be able to miniaturize two consecutive modes of the rectangular patch antenna that could be employed in arraying. As a trade-off, the bandwidth of the present study has narrow bandwidth characteristics compared to other studies given in the Table since the antenna is a resonance-type antenna. however, the proposed antenna aims to be employed in indoor Wi-Fi applications, therefore; the wide bandwidth is not required.

TABLE 2. Comparison with Several Studies.

Ant.	Ctr. Freq.	Size in mm	$\lvert S_{11}\rvert$ (in dB)	Approach
[16]	2.45 GHz	45×45	-18	multimode
[22]	3.6 GHz	34×34×1.525	-	multimode
[23]	5.1 GHz	49.64×49.64×0.75	-9	multimode
[25]	5.5 GHz	20×15×0.26	-12	stub, fractal
[26]	40 GHz	12.5×12.5×1.12	-14	E-shaped patch
[27]	10.5 GHz	25×11.9×2.5	-10	aperture
Study	2.45 GHz	37.4×35.5×1.6	-11	multimode

III. SIMULATION AND EXPERIMENTAL RESULTS

To confirm and validate the operation of the design, a prototype antenna is manufactured, and measurements are conducted on this prototype. The patch antennas are fabricated by employing the LPKF H100 Promat prototyping machine. Fabrication is done by milling out undesired parts from the conducting sheet. The feeding is done with a coaxial probe with 50 Ω impedance. The prototype antenna is realized with SMA connectors. Apart from the scattering parameters, radiation patterns and maximum gain values of the antenna are also measured. These measurements are conducted at the anechoic chamber at the Middle East Technical University, Antennas, and Microwave Laboratory. In Figures 7 and 8 manufactured prototype of the antenna and measurement set-up in the anechoic chamber can be seen.

To understand the antenna's resonance behavior, $|S_{11}|$ measurements are conducted. Measurements are conducted via a Vector Network Analyzer (Keysight E5071C). The measurement results and their comparison with the simulations of $|S_{11}|$ and $|S_{22}|$ can be seen in Figures 9 and 10. In these measurements, only a single antenna port is connected to the network analyzer, while the other port is terminated with a matched load.

As it can be seen from Figure 9 and 10, both antennas resonate at 2.45 GHz. The measurement and simulation

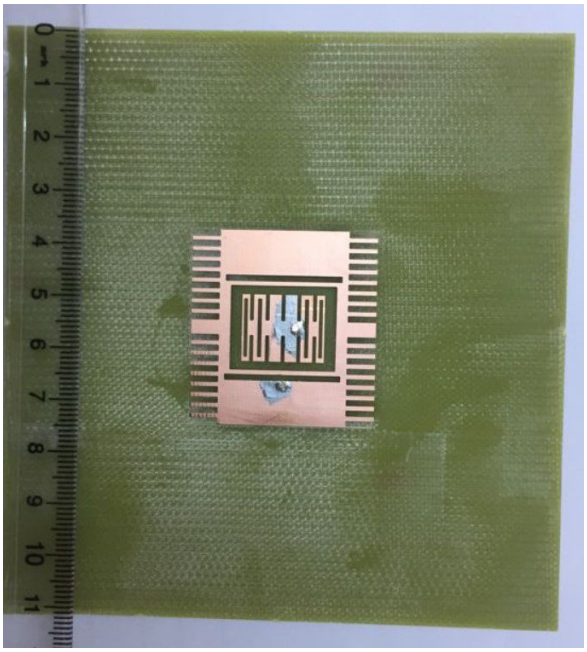

FIGURE 7. Top view of the fabricated prototype.

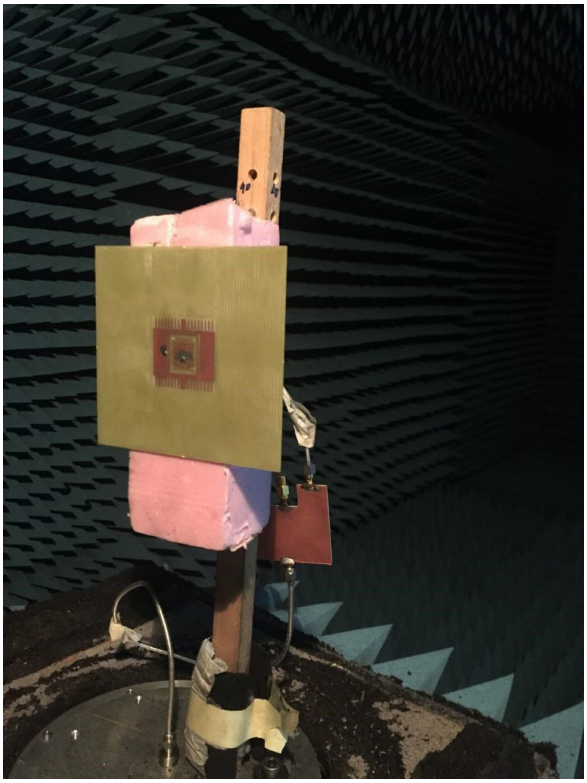

FIGURE 8. Produced antenna (a): top view (b) anechoic chamber set-up.

results are in coherence. A minor frequency shift is observed at $|S_{22}|$ value. The fabricated antenna resonates at 0.015 GHz higher frequency than the designed one. Fabrication errors can explain this frequency shift. There was a fabrication

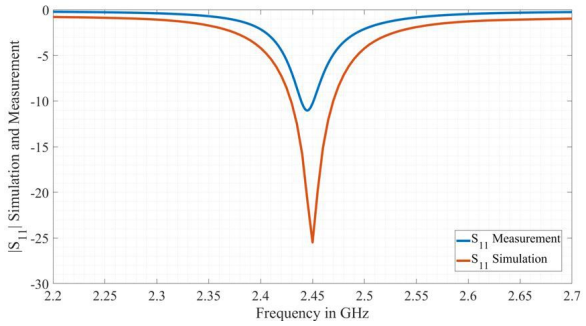

FIGURE 9. $|S_{11}|$ value of the antenna (in dB).

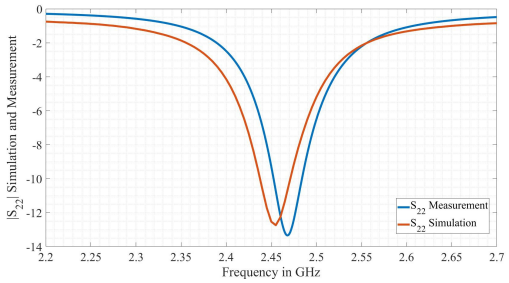

FIGURE 10. $|S_{22}|$ value of the antenna (in dB).

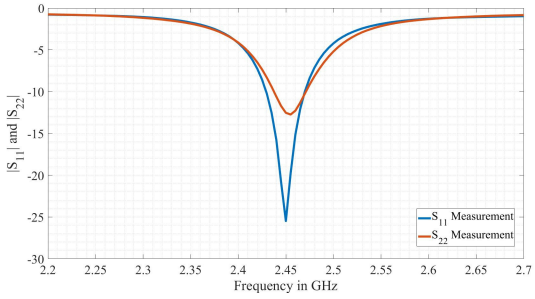

FIGURE 11. Measurements of $|S_{11}|$ and $|S_{22}|$ in dB.

challenge at the last fractal elements of the outer rectangular antenna as the size of these elements is very small compared to other fractal elements. Due to these factors, the resonance point of the outer antenna is shifted slightly towards higher frequencies. The scattering parameters of the two-port operation of the antenna can be observed from Figure 11.

The isolation value of the antenna is provided in Figure 12. As can be seen from the figure, the $|S_{21}|$ simulation value of the antenna is always smaller than -15 dB in the operating frequency, which is more than enough to have an efficient radiation phenomenon.

The antenna supports three different excitation pairs. In the first two cases, only one antenna element is fed, and the other element is connected to matched termination. The measurement results of these cases and their comparison with the simulation can be found in Figures 13 to 15.

In radiation pattern figures, the antenna is placed at the x-z

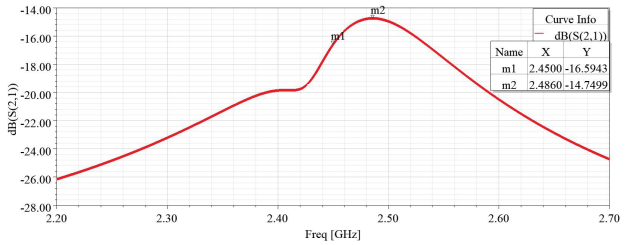

FIGURE 12. $|S_{21}|$ values of the antenna.

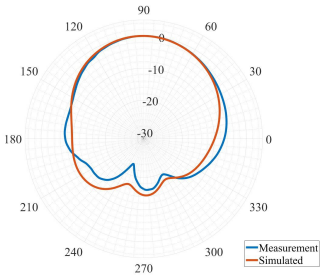

FIGURE 13. Radiation patterns (in dB) of the antenna in the y-z (elevation) plane: (TM_{01}) operation with the inner element (2.45 GHz)

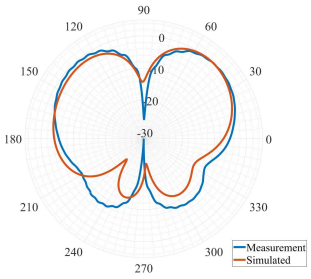

FIGURE 14. Radiation patterns (in dB) of the antenna in the y-z (elevation) plane: (TM_{02}) operation with the outer element (2.45 GHz).

plane. Therefore radiation towards 90^0 illustrates broadside radiation. The broadside (TM_{01}) and conical beam (TM_{02}) radiation characteristics are clearly seen in Figure 13 and 14, respectively. In the third measurement given in Figure 15, the antenna is fed by unequal input powers as mentioned in Section II. To have an almost flat radiation pattern, the input power of the inner element is reduced by 3 dB compared to the outer element.

As shown in Figure 15, the operation of two modes simultaneously results in an almost flat radiation pattern within a very large beam width. The 1 dB beamwidth of the measured prototype antenna is found as 95^0. All of the radiation pattern measurements agree with the simulation outcomes. The maximum gain of the antenna when ports are operated simultaneously is measured as -6.41 dB. The maximum gain value of the same scenario is simulated as -6.32 dB. The difference between simulation and measurement is tiny, and it is caused by the additional conduction losses introduced by the welding procedure.

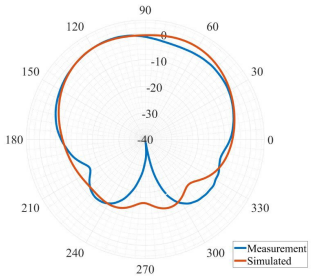

FIGURE 15. Radiation pattern (elevation plane) of the antenna (in dB) when two ports are operated simultaneously (2.45 GHz).

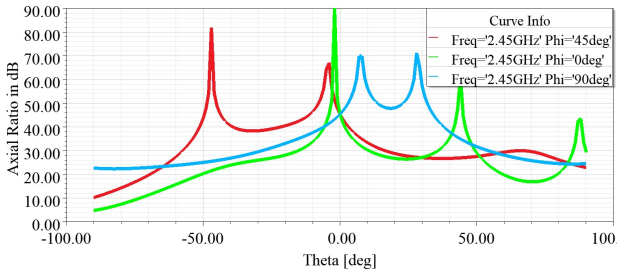

FIGURE 16. Axial Ratio plots belonging to different ϕ cuts (45^0,$0^0$and 90^0) at 2.45 GHz.

This antenna employs two orthogonal radiators to form a constant gain element. As two orthogonal elements are used to form a pattern, the polarization orientation of the element is rotated to roughly $\phi = 45^0$. This antenna is designed to operate in IoT applications; therefore, there would always be an excessive amount of reflections and multipath. Since the signal experiences multiple reflections, polarization sense would be the essential parameter of the polarization rather than the direction. The designed antenna has linear polarizatıon, so its polarization directıon ($\phi = 45^0$) does not have prior importance for indoor applications. Although the polarization direction is rotated, the antenna achieves linear polarization. The axial ratio simulations of the antenna at $\phi = 45^0$, $\phi = 0^0$, and $\phi = 90^0$ cuts can be seen in Figure 16. As can be seen from this figure, the axial ratio values at three major cuts stay above 20 dB in the desired θ scan range.

As a final remark, it can be said that the antenna achieves 90^0 beam width by spanning $\pm 45^0$ interval in elevation. To satisfy this goal, monopole-like radiation is necessary. However, having only monopole-like radiation reduces the amount of the radiated beam to the broadside. This reduction is balanced with an additional radiating mechanism where the main beam is at the broadside. In other words, Monopole-like (conical beam) radiation is obtained by exiting TM_{02} while broadside radiation is achieved by TM_{01} mode excitement. These two modes are needed to be superposed to have a constant radiation pattern within the proposed range at the same operating frequency. Their phase center should be the same to superpose different TM modes constructively. These requirements yield a co-centric rectangular patch structure

excited by different modes. When the gain values of TM_{01} and TM_{02} modes are investigated, approximately a 3 dB difference is observed. Unequal amplitude weightings solve this problem for each radiator. Two different antenna miniaturization techniques are utilized since the design is initially planned to be employed in the array structure. These miniaturization techniques are slot employment and fractalization of non-radiating edges. To avoid grating lobes, the distance between the consecutive elements should be less than half the free-space wavelength of the operating frequency. Positioning the radiators in a co-centric manner results in coupling problems. This problem is solved by rotating radiating edges of the antennas to make a 90^0 angle.

IV. CONCLUSION

The present study developed a multi-mode pattern diverse microstrip patch antenna with a constant gain in the elevation plane. The present study can be distinguished from previous studies concerning the following aspects. The study introduces the possible usage of the multi-pattern antenna in indoor applications. These usage areas become possible by presenting extra broad beam antennas. Extra broad beam corresponds to having more than 90^0 beamwidth (1 dB beamwidth). In order to achieve this goal, two independent resonators are used simultaneously. Two different approaches for miniaturization are employed in design to construct an array. Having multiple resonators causes an isolation and coupling problem. A simple and novel solution eliminates this problem: aligning the radiating edges perpendicular to each other.

The design aims to provide Wi-Fi users equitable service with a predefined angle range. Therefore, the operating frequency is selected in the free band region of the S-band. The pattern-diverse antenna structures are an appealing solution to all of these design goals. The design aims to achieve an antenna element capable of providing a broad beam radiation pattern covering more than 90^0 in the elevation plane. Multi-pattern structures are easy to realize on the microstrip antennas. Therefore, TM_{01} and TM_{02} modes are selected for the present study.

ACKNOWLEDGMENT

The authors of the paper would like to express their gratitude to İrem Bozkurt, Damla Alptekin Soydan, and Prof. Dr. Özlem Aydın Çivi. This work is supported in part by Istanbul Technical University (ITU) Vodafone Future Lab under Project No. ITUVF20180901P10.

REFERENCES

[1] F. T. Çelik and K. Karaçuha, "Miniaturized virtual array dual band loop quasi – yagi antenna design for 5g application," in 2019 URSI International Symposium on Electromagnetic Theory (EMTS), pp. 1–4, 2019.

[2] F. T. Çelik and K. Karaçuha, "A reconfigurable binomial weighted phased array antenna design for wi-fi band," in 2020 28th Signal Processing and Communications Applications Conference (SIU), pp. 1–4, 2020.

[3] F. T. Çelik, "Pattern reconfigurable antenna designs in sub-6 ghz band for 5g applications," Master's thesis, Middle East Technical University, 2021.

[4] A. Pal, A. Mehta, D. Mirshekar-Syahkal, and H. Nakano, "A twelve-beam steering low-profile patch antenna with shorting vias for vehicular applications," IEEE Transactions on Antennas and Propagation, vol. 65, no. 8, pp. 3905–3912, 2017.

[5] L. C. Paul, S. C. Das, N. Sarker, R. Azim, M. F. Ishraque, and S. A. Shezan, "A wideband microstrip patch antenna with slotted ground plane for 5g application," in 2021 International Conference on Science Contemporary Technologies (ICSCT), pp. 1–5, 2021.

[6] K. Mazen, A. Emran, A. S. Shalaby, and A. Yahya, "Design of multi-band microstrip patch antennas for mid-band 5g wireless communication," International Journal of Advanced Computer Science and Applications, vol. 12, no. 5, 2021.

[7] D. A. J. Al-Khaffaf and I. A. Alshimaysawe, "Miniaturised tri-band microstrip patch antenna design for radio and millimetre waves of 5g devices," Indonesian Journal of Electrical Engineering and Computer Science, vol. 21, no. 3, pp. 1594–1601, 2021.

[8] S. Zhang, G. Huff, J. Feng, and J. Bernhard, "A pattern reconfigurable microstrip parasitic array," IEEE Transactions on Antennas and Propagation, vol. 52, no. 10, pp. 2773–2776, 2004.

[9] S. Preston, D. Thiel, J. W. Lu, S. O'keefe, and T. Bird, "Electronic beam steering using switched parasitic patch elements," Electronics Letters, vol. 33, no. 1, pp. 7–8, 1997.

[10] Y. Cao, Y. Cai, W. Cao, Z. Qian, and L. Zhu, "Wideband microstrip patch antenna loaded with parasitic metal strips and coupling slots," IEICE Electronics Express, vol. 15, no. 15, pp. 1–8, 2018.

[11] C. D. Erbaş, "Parametric analysis of angular rotation for microstrip patch antenna with elliptical patch and parasitic elements," in 2020 International Conference on Electrical, Communication, and Computer Engineering (ICECCE), pp. 1–6, IEEE, 2020.

[12] F. T. Celik and K. Karacuha, "A conical-beam dual-band double aperture-coupled stacked elliptical patch antenna design for 5g," Turkish Journal of Electrical Engineering and Computer Sciences, vol. 30, no. 6, pp. 2073–2085, 2022.

[13] S. Liu, W. Wu, and D.-G. Fang, "Wideband monopole-like radiation pattern circular patch antenna with high gain and low cross-polarization," IEEE Transactions on Antennas and Propagation, vol. 64, no. 5, pp. 2042–2045, 2016.

[14] S.-H. Chen, J.-S. Row, and K.-L. Wong, "Reconfigurable square-ring patch antenna with pattern diversity," IEEE Transactions on Antennas and Propagation, vol. 55, no. 2, pp. 472–475, 2007.

[15] J. Liu, Q. Xue, H. Wong, H. W. Lai, and Y. Long, "Design and analysis of a low-profile and broadband microstrip monopolar patch antenna," IEEE Transactions on Antennas and Propagation, vol. 61, no. 1, pp. 11–18, 2012.

[16] S. Dumanli, "Pattern diversity antenna for on-body and off-body wban links," Turkish Journal of Electrical Engineering and Computer Sciences, vol. 26, no. 5, pp. 2395–2405, 2018.

[17] F. T. Celik, L. Alatan, and O. A. Civi, "A compact pattern reconfigurable antenna employing shorted quarterwave patch antennas," Turkish Journal of Electrical Engineering and Computer Sciences, vol. 30, no. 6, pp. 2179–2189, 2022.

[18] T. A. Morgado, J. M. Alves, J. S. Marcos, S. I. Maslovski, J. R. Costa, C. A. Fernandes, and M. G. Silveirinha, "Spatially confined uhf rfid detection with a metamaterial grid," IEEE Transactions on Antennas and Propagation, vol. 62, no. 1, pp. 378–384, 2013.

[19] G.-M. Zhang, J.-S. Hong, B.-Z. Wang, G. Song, and P. Li, "Design and time-domain analysis for a novel pattern reconfigurable antenna," IEEE Antennas and Wireless Propagation Letters, vol. 10, pp. 365–368, 2011.

[20] H.-W. Yu, Y.-C. Jiao, D.-Y. Li, and Z.-B. Weng, "A tm 30-/tm 40-mode pattern-reconfigurable microstrip patch antenna for wide beam coverage," IEEE Transactions on Antennas and Propagation, vol. 67, no. 11, pp. 7121–7126, 2019.

[21] F. T. Çelik, L. Alatan, and A. Çivi, "A pattern reconfigurable compact antenna structure based on shorted microstrip patches," in 2022 16th European Conference on Antennas and Propagation (EuCAP), pp. 1–4, 2022.

[22] F. T. Çelik, L. Alatan, and O. A. Civi, "A pattern reconfigurable multi-mode antenna based on circular disk and ring-shaped resonators," in 2022 IEEE International Symposium on Antennas and Propagation and USNC-URSI Radio Science Meeting (AP-S/URSI), pp. 405–406, IEEE, 2022.

[23] T. Q. Tran and S. K. Sharma, "Radiation characteristics of a multimode concentric circular microstrip patch antenna by controlling amplitude and phase of modes," IEEE Transactions on Antennas and Propagation, vol. 60, no. 3, pp. 1601–1605, 2011.

[24] C. A. Balanis, Antenna Theory: Analysis and Design. John wiley & sons, 2015.

[25] W. A. Awan, M. Husain, M. Alibakhshikenari, and E. Limiti, "Band enhancement of a compact flexible antenna for wlan, wi-fi and c-band applications," in 2021 International Symposium on Antennas and Propagation (ISAP), pp. 1–2, IEEE, 2021.

[26] J. Yin, Q. Wu, C. Yu, H. Wang, and W. Hong, "Broadband symmetrical e-shaped patch antenna with multimode resonance for 5g millimeter-wave applications," IEEE Transactions on Antennas and Propagation, vol. 67, no. 7, pp. 4474–4483, 2019.

[27] M. Bilgic and K. Yegin, "Wideband offset slot-coupled patch antenna array for x/ku-band multimode radars," IEEE Antennas and Wireless Propagation Letters, vol. 13, pp. 157–160, 2014.